An Optimal Control Strategy Separating Two Species of Microalgae in Photobioreactors

Walid Djema, Laetitia Giraldi, Olivier Bernard

An Optimal Control Strategy Separating Two Species of Microalgae in Photobioreactors ⋆

Walid Djema [*,**] **Laëtitia Giraldi** [**] **Olivier Bernard** [*]

[*] *BIOCORE Project team, Inria Sophia Antipolis Mediterranean, Côte d'Azur University (UCA), France.*
[**] *McTAO Project team, Inria Sophia Antipolis Mediterranean, Côte d'Azur University (UCA), France.*
walid.djema@inria.fr, laetitia.giraldi@inria.fr, olivier.bernard@inria.fr

Abstract: We investigate a minimal-time control problem in a chemostat continuous photobioreactor model that describes the dynamics of two distinct microalgae populations. More precisely, our objective in this paper is to optimize the time of selection – or separation – between two species of microalgae. We focus in this work on Droop's model which takes into account an internal quota storage for each microalgae species. Using Pontryagin's principle, we develop a dilution-based control strategy that steers the model trajectories to a suitable target in minimal time. Our study reveals that singular arcs play a key role in the optimization problem. A numerical optimal-synthesis, based on direct optimal control tools, is performed throughout the paper, thereby confirming the optimality of the provided feedback-control law, which is of type *bang-singular*.

Keywords: Optimization, feedback control, nonlinear, Droop's model, microalgae, chemostat.

1. INTRODUCTION

The principle of competitive exclusion (Hsu & *et al.* (1977)) states that one of the species wins the competition to the detriment of others. This concept has been widely used in ecology, but more rarely applied in biotechnology, with the objective of eventually improving the quality and the productivity of some products (e.g. food and fuel). In the case of microorganisms, the selection of species of interest can be achieved through a competition process taking place in continuous cultures (Liu (2016), Chap. 12).

The chemostat is a continuous reactor dedicated to growth of microorganisms. It is also an environment in which the principle of competition occurs either between different species of microorganisms initially coexisting, or within one pool of stains in the same species that becomes subsequently divided into several sub-populations. A basic modeling framework is known as the Monod's model, which is the mostly used representation of microorganisms growing inside the chemostat (Monod (1942, 1950)). Standard properties derive from analysis of the Monod's model, as the *competitive exclusion principle* (CEP) that describes the basics of competition in chemostat (see e.g. Smith & Waltman (1995)). The CEP predicts that if several species are introduced in the chemostat, the one that requires the less nutrient to sustain a growth rate equal to the dilution rate will win the competition, while the other species will vanish out asymptotically (Smith & Waltman (1995); Hsu (2008)). Not surprisingly, a great importance is given to the issue of controlling the chemostat system in order to select differently the species that wins the competition, according to more attractive and practical criteria (Masci *et al.* (2008), but see also Grognard *et al.* (2015) and Mazenc & Malisoff (2010), in particular for situations where co-existence between different species is of interest).

More recently, some approaches based on optimal control theory have been applied to Monod's model, in order to drive and accelerate the CEP, leading to species selection in *finite time* (Bayen & Mairet (2014, 2017)). Unfortunately, the application of optimal control techniques in microalgae, which are more complex systems (see e.g. Bernard (2011); Bernard *et al.* (2015)), appears to be a challenging issue. Indeed, microalgae are particular microorganisms that have the ability to store internally the substrate before using it for growth. These storage mechanisms cannot be captured by the classical Monod's model, and a more suitable framework for microalgae growth is provided by the so-called Droop's model (Droop (1973, 1968, 1983); Smith & Waltman (1995); Hsu (2008)). More precisely, Droop's model includes a new dynamics where an internal nutrient storage is introduced, so that only nutrients internal to the cell are available for cell growth. In fact, this additional state variable needs to describe the uptake of nutrients (Caperon & Meyer (1972)) in cell (see Figure 1). Notice that Droop's model is also known as the variable yield model, as it no longer assumes a constant ratio between cell growth and nutrient consumption rate (Smith & Waltman (1995)). Finally, it is worth mentioning that, from a mathematical standpoint, the cell-quota dynamics increases the overall dimension of the model, as well as the resulting difficulty in the mathematical analysis.

⋆ This work was supported by the *IPL Algae in silico*, Inria Project Lab, France.

This work is devoted to the analysis of a competition model with two species described with a Droop kinetics. This can be seen as a generalisation of the approach of Bayen & Mairet (2014), with a more complex class of systems involving two additional states (i.e. the internal quota of each species). The paper is organized as follows: Droop's model is introduced in Section 2 and the optimal control problem of interest is stated in Section 3. Pontryagin's principle is applied in Section 4, and a numerical optimal synthesis is carried out in Section 5.

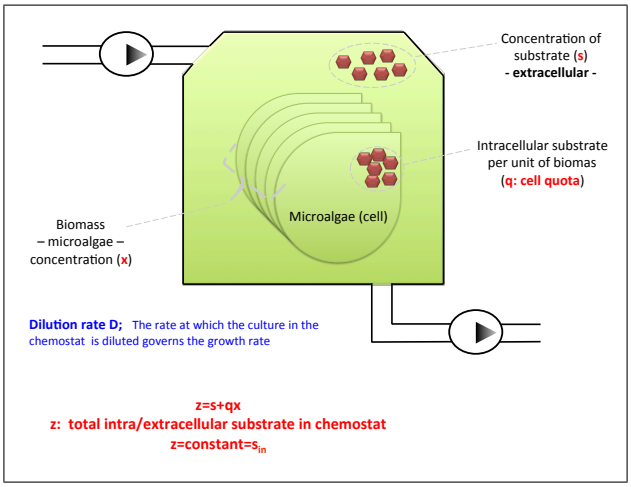

Fig. 1. Schematic representation of a chemostat, which is an open reactor that keeps a cell culture at a specific volume, adds continuously fresh medium while removing spent culture. The figure introduces basic notations in the case of one species.

2. THE MATHEMATICAL MODEL

A microalgae species concentration x_i, where $i = 1, 2$, consumes a nutriment s and transforms it into internal storage q_i. In fact, x_1 and x_2 can be seen as different species or stains coexisting in a chemostat with one limiting substrate s. The cell quota q_i increases with nutrient absorption and decreases with cell proliferation, since cell division spreads the total quantity of stored nutrient over more cells. In fact, the total amount of stored nutrient at time $t \geq 0$ is given by $\sum_{i=1}^{2} q_i(t)x_i(t)$.

The variable yield model – Droop's model – involving two species is described by:

$$\begin{cases} \dot{s} = (s_{in} - s)D - \sum_{i=1}^{2} \rho_i(s)x_i, \\ \dot{q}_i = \rho_i(s) - \mu_i(q_i)q_i, \\ \dot{x}_i = [\mu_i(q_i) - D]\, x_i, \end{cases} \tag{1}$$

where $i = 1, 2$, the total substrate concentration s is a scalar variable, and s_{in} is the constant input concentration of the substrate. As previously mentioned, x_i is the i-th species-biomass concentration, and q_i is the internal substrate storage for the i-th species. The dilution rate is denoted D. In experiment, it is usual to play on D, which is indeed a bounded nonnegative control in system (1). Next, ρ_i is a real-valued function quantifying the rate of substrate absorption, i.e. the uptake rate of free nutriment s; while μ_i is a real-valued function quantifying the growth rate of the i-th species. The functions ρ_i and μ_i are nonnegative and increasing bounded functions, s.t.,

$$0 \leq \rho_i(s) \leq \rho_{mi}, \quad 0 \leq \mu_i(q_i) \leq \mu_{mi}, \tag{2}$$

where ρ_{mi} and μ_{mi} are strictly positive constants. In fact, typically in Droop's model, the uptake rate $\rho_i(s)$ is expressed in terms of Michaelis-Menten kinetics:

$$\rho_i(s) = \frac{\rho_{mi} s}{K_{si} + s}, \tag{3}$$

where K_{si} is a strictly positive constant of the i-th species.

We consider that there exists a minimum threshold $k_{qi} > 0$, for each species, under which cell division cannot occur, and we consider the growth rates in the Droop's form:

$$\mu_i(q_i) = \mu_{i\infty}\left(1 - \frac{k_{qi}}{q_i}\right), \quad q_i \geq k_{qi}. \tag{4}$$

In fact, we can see that for all $t \geq 0$, $k_{qi} \leq q_i(t) \leq q_{mi}$, where q_{mi} is the maximum internal storage rate, and $\mu_{i\infty} = \frac{q_{mi}}{q_{mi} - k_{qi}}\mu_{mi}$, with $\lim_{q_i \to +\infty} \mu_i(q_i) = \mu_{i\infty}$.

For each fixed $s = s_*$, i.e. under a constant substrate concentration s_*, we notice that q_i converges towards $q_i(s_*)$, which is the unique and attractive solution of the equation $\mu_i(q_i(s_*))q_i(s_*) = \rho_i(s_*)$, for $i = 1, 2$. In addition, to be consistent with inequalities (2), we have:

$$\rho_{mi} = \mu_i(q_{mi})q_{mi}, \tag{5}$$

where q_{mi} is the maximum internal storage rate previously defined, and $\mu_i(q_{mi})$ corresponds to the maximum growth rate for the i-th species, i.e. $\mu_i(q_{mi}) = \frac{\rho_{mi}}{q_{mi}} = \mu_{mi}$.

Clearly, the system (1) is positive, i.e. for strictly positive initial conditions the trajectories remain positive. The total mass in the chemostat system is given by: $z = s + q_1x_1 + x_2q_2$. The following statement allows us to reduce the dimension of the studied system:

Proposition 1. The set,

$$\mathcal{F} = \{(s, q_1, q_2, x_1, x_2) \in \mathbb{R}_+^* \times \mathbb{R}_+^* \times \mathbb{R}_+^* \times \mathbb{R}_+^* \times \mathbb{R}_+^* | \\ k_{qi} \leq q_i \leq q_{im}, \ q_1x_1 + q_2x_2 + s = s_{in}\},$$

is invariant and attractive for system (1).

Indeed, standard arguments show that the total mass remains constant, $z = s_{in}$, when the initial conditions are within $\mathcal{F}$ (the conservation principle, Smith & Waltman (1995), Chap. 8, Sect. 4). More precisely, to see why Proposition 1 holds, it is sufficient to notice that z satisfies, along the trajectories of system (1), the dynamics:

$$\dot{z} = (s_{in} - z)D,$$

where the dilution rate D is assumed to not be identically zero for all future time. As a consequence, considering that the initial conditions associated to system (1) belong to the set $\mathcal{F}$ allows us to reduce the dimension of system (1), since $s = s_{in} - q_1x_1 - q_2x_2$ for all future time, as formulated in the next section.

Now, before stating the optimal control problem, let us define some useful functions and constants. Using the forms of the functions ρ_i and μ_i, given respectively in (3) and (4), we readily get $\rho_i^{-1}(a) = \frac{K_{si}a}{\rho_{im} - a}$, $\rho_i^{-1} : [0, \rho_{im}) \to [0, +\infty)$, and we define the function:

$$\delta_i(a) = \rho_i^{-1}(\tilde{\mu}_i(a)) = K_{si}\frac{a - k_{qi}}{\kappa_i - a}, \quad a \in [0, \kappa_i),$$

where, $\tilde{\mu}_i(a) = \mu_i(a)a$, and, $\kappa_i = \frac{\rho_{im}}{\mu_{i\infty}} + k_{qi}$. In fact, we notice that if we regulate the substrate s to a fixed value $s_* \in [0, s_{in}]$, then the quota q_i is regulated to the unique value, $q_i(s_*)$, satisfying $\rho_i(s_*) = \tilde{\mu}_i(q_i(s_*))$, or, equivalently, $s_* = \delta_i(q_i(s_*))$, for $i = 1, 2$, since all the functions are bijective (we recall that $q_i \geq k_{qi}$). This means that the elemental cell quota, and which are directly available for cell growth of each species, are approaching the values: $q_i(s_*) = \delta_i^{-1}(s_*)$, for $i = 1, 2$, where,

$$\delta_i^{-1}(s_*) = \frac{\kappa_i s_* + K_{si} k_{qi}}{s_* + K_{si}}.$$

Thus, we can define the effective growth rate of each species with respect to $q_i(s_*)$:

$$\mu_i(q_i(s_*)) = \mu_i(\delta_i^{-1}(s_*)) = \frac{\rho_{im} s_*}{\kappa_i s_* + K_{si} k_{qi}}. \tag{6}$$

The function $\mu_i(q_i(s))$ is increasing for all $s \in [0, s_{in}]$. In light of the above arguments about the effective growth rate of each species, we expect at a first sight that the maximization – or minimization – of the function:

$$\Delta(s) = \mu_1(\delta_1^{-1}(s)) - \mu_2(\delta_2^{-1}(s)), \tag{7}$$

along a feasible trajectory $s(t)$, for all $t \geq 0$, solution of system (1), plays a role in the optimal strategy separating between the involved species. To see why, observe that the optima of the function $\Delta(s)$ represent the operating modes with the largest gap between potential growth of the species. Hence, for later use, we denote $s_c \in [0, s_{in}]$ the constant that maximizes the function $\Delta(s)$. The functions discussed above are illustrated in Figure 2.

3. STATEMENT OF THE OPTIMAL CONTROL PROBLEM

Now, we want to formulate the optimal control problem (OCP) of interest in this paper. Firstly, we recall from the previous section that we can limit ourselves to the trajectories of system (1) that are confined in the invariant set $\mathcal{F}$. Thus, we leave aside the s-dynamics and we introduce for system (1) the – biologically relevant – set:

$$\mathcal{S} = \{(q_1, q_2, x_1, x_2) \in \mathbb{R}_+^* \times \mathbb{R}_+^* \times \mathbb{R}_+^* \times \mathbb{R}_+^* \mid k_{qi} \leq q_i \leq q_{im},\ q_1 x_1 + q_2 x_2 < s_{in}\}.$$

Then, next, we define the target $\mathcal{T}$ of interest as follows:

$$\mathcal{T} = \{X := (q_1, q_2, x_1, x_2) \in \mathcal{S} \ \mid \ x_2 < \epsilon x_1\},$$

where X satisfies system (1), $X(0) \in \mathcal{F}$, and ϵ is a small enough strictly positive constant. In fact, we are assuming that the species x_1 is the one of interest from a biological standpoint. Thus, the target $\mathcal{T}$ expresses a situation where the concentration of the first species is significantly larger than the second one, with a small ϵ that represents the final contamination rate of the selected population x_1.

Our objective is to determine a dilution-based optimal control strategy D that allows the trajectories of system (1), starting from arbitrary initial conditions within $\mathcal{F}$, to reach the target $\mathcal{T}$ in minimal time. For that, we define firstly the set of admissible controls:

$$\mathcal{D} = \{D : [0, +\infty] \to [0, D_{\max}] \ \mid \ D(\cdot) \in \mathcal{L}^\infty_{loc}(\mathbb{R}^+)\},$$

where $D_{\max}$ is a sufficiently large strictly positive constant. Thus, $\mathcal{D}$ is a subset of $\mathcal{L}^\infty_{loc}(\mathbb{R}^+)$, the space of locally integrable functions on every compact on $\mathbb{R}^+$.

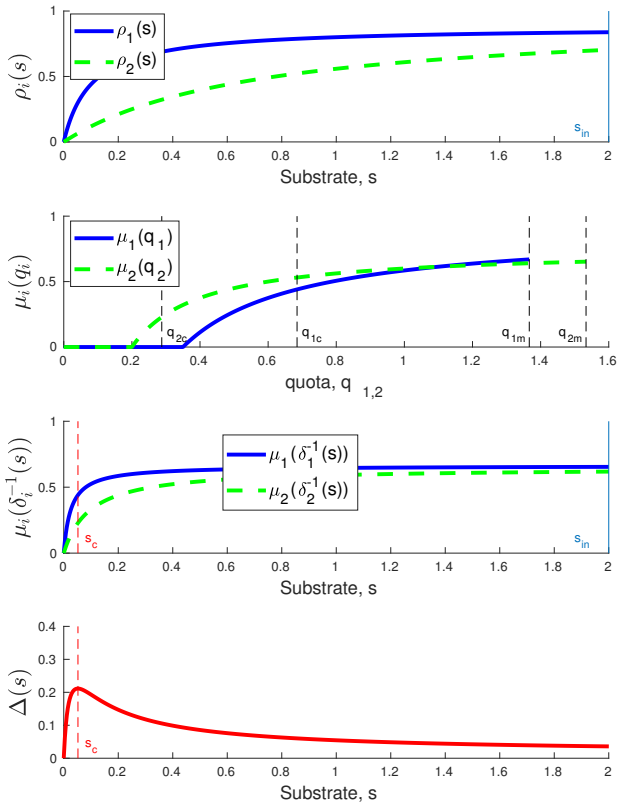

Fig. 2. Illustrations of the functions $\rho_i(\cdot)$, $\mu_i(\cdot)$ and $\mu_i(\delta_i^{-1}(\cdot))$. The constant $s_c = 0.0520$ maximizes the function $\Delta(s)$, $\forall s \in [0, s_{in}]$, with $s_{in} = 2$; $q_{ic} = q_i(s_c)$. The corresponding numerical values of the biological parameters are provided in Section 5 (Table 1).

The optimal control problem (OCP) of interest is stated as follows. For all initial conditions [1] belonging to $\mathcal{F}$, we are seeking for an admissible control strategy $D \in \mathcal{D}$, steering the solution $X = (q_1, q_2, x_1, x_2)$ of the reduced system,

$$\begin{cases} \dot{q}_i = \rho_i(s) - \mu_i(q_i) q_i, \\ \dot{x}_i = [\mu_i(q_i) - D]\, x_i, \end{cases} \tag{8}$$

where $i = 1, 2$, and $s = s_{in} - q_1 x_1 - q_2 x_2$, to the target set $\mathcal{T}$ in minimal time, i.e., for a fixed $D_{\max}$ and a given contamination rate ϵ, the OCP reads,

$$\begin{aligned} &\inf_{D \in \mathcal{D}} t_f, \quad \text{s.t.} \quad X(t_f) \in \mathcal{T}, \\ &X(\cdot) \text{ is solution of (8)}, \quad \text{and} \quad X(0) \in \mathcal{F}. \end{aligned} \tag{9}$$

Standard arguments allow us to establish that, under reasonable conditions, there exists at least one control that steers any initial conditions within $\mathcal{F}$ to the target $\mathcal{T}$. Indeed, firstly we observe that a fixed control D selects asymptotically – through the CEP – one species, that we assume to be x_1. We note that the steady state $(\overline{x}_1, \overline{x}_2)$ where $\overline{x}_1 > 0$, $\overline{x}_2 = 0$ belongs to $\mathcal{T}$. Thus, since $(\overline{x}_1, \overline{x}_2)$ is asymptotically stable, we deduce that for any $\epsilon > 0$, the fixed control D steers the trajectories into $\mathcal{T}$ in finite time.

Now, we are in position to apply Pontryagin's principle (Pontryagin *et al.* (1964)) in order to provide necessary conditions for the optimality of the control D that we want to determine.

[1] We note that any initial condition within $\mathcal{F}$ also belongs to $\mathcal{S}$.

4. APPLICATION OF THE PONTRYAGIN MAXIMUM PRINCIPLE

Let $H = H(q_1, q_2, x_1, x_2, \lambda_1, \lambda_2, \lambda_3, \lambda_4, \lambda_0, D)$ be the Hamiltonian of the reduced system (8) associated with the OCP given in (9), that is:

$$\begin{aligned} H =&(\rho_1(s) - \mu_1(q_1)q_1)\lambda_1 + (\rho_2(s) - \mu_2(q_2)q_2)\lambda_2 \\ &+ \mu_1(q_1)x_1\lambda_3 + \mu_2(q_2)x_2\lambda_4 + \lambda_0 + D\Phi, \end{aligned} \tag{10}$$

where,

$$\Phi = -\lambda_3 x_1 - \lambda_4 x_2, \tag{11}$$

the λ_is are the co-states of q_1, q_2, x_1 and x_2, governed by:

$$\dot\lambda_1 = -\frac{\partial H}{\partial q_1}, \;\; \dot\lambda_2 = -\frac{\partial H}{\partial q_2}, \;\; \dot\lambda_3 = -\frac{\partial H}{\partial x_1}, \;\; \dot\lambda_4 = -\frac{\partial H}{\partial x_2}, \tag{12}$$

and the states of the reduced system (8) satisfy:

$$\dot q_1 = \frac{\partial H}{\partial \lambda_1}, \;\; \dot q_2 = \frac{\partial H}{\partial \lambda_2}, \;\; \dot x_1 = \frac{\partial H}{\partial \lambda_3}, \;\; \dot x_2 = \frac{\partial H}{\partial \lambda_4}, \tag{13}$$

with $X(0) \in \mathcal{F}$. It is classical to set $\lambda_0 = -1$ in minimization problems. Next, in Pontryagin's approach, the control D satisfies the maximization condition: $D(t) \in \operatorname{argmax}_{D\in[0,D_{\max}]} H(q_1, q_2, x_1, x_2, \lambda_1, \lambda_2, \lambda_3, \lambda_4, \lambda_0, D)$, for almost all $t \geq [0, t_f]$, where t_f is the first time the trajectories reach the target. Thus, since the Hamiltonian is linear with respect to the control, we deduce that the control law is given by the sign of the switching function Φ, that is:

- $D = D_{\max}$ iff $\Phi > 0$.
- $D = 0$ iff $\Phi < 0$.
- $D = D_c$, when $\Phi = 0$ (D_c is called the singular control, and it will be determined in the rest).

Before determining the singular control D_c, let us express the transversality conditions of the optimization problem. By definition, the co-state vector satisfies [2] at $t = t_f$,

$$[\lambda_1(t_f)\ \lambda_2(t_f)\ \lambda_3(t_f)\ \lambda_4(t_f)]^{tr} \in \mathcal{N}_{\mathcal{T}}(X(t_f)), \tag{14}$$

where $X = (q_1, q_2, x_1, x_2)$ is solution of (8) and $\mathcal{N}_{\mathcal{T}}$ is the normal cone to the target $\mathcal{T}$ at the point $X(t_f)$. Hence,

$$[\lambda_1(t_f)\ \lambda_2(t_f)\ \lambda_3(t_f)\ \lambda_4(t_f)] \begin{bmatrix} 1 & 0 & 0 \\ 0 & 1 & 0 \\ 0 & 0 & 1 \\ 0 & 0 & \epsilon \end{bmatrix} = 0. \tag{15}$$

In particular, from the definition of the target $\mathcal{T}$, the system (15) expresses that $[\lambda_3(t_f)\ \lambda_4(t_f)]^{tr}$ is parallel to the vector $\boldsymbol{v} = [\epsilon\ -1]^{tr}$. In other words, there exists α, s.t., $[\lambda_3(t_f)\ \lambda_4(t_f)]^{tr} = \alpha v$. Therefore, it follows that:

$$\Phi(t_f) = -\,\alpha\,[\epsilon\ -1] \begin{bmatrix} x_1(t_f) \\ x_2(t_f) \end{bmatrix} = 0. \tag{16}$$

We conclude that the target $\mathcal{T}$ is reached with the singular control D_c.

Now, we want to determine the explicit form of the singular control D_c. Thanks to the numerical optimal synthesis that we perform on Droop's model (through direct methods, as developed in the next section), we note that the singular control D_c is activated on a time-interval that is not reduced to a point. So, let us consider that the function Φ, defined in (11), is vanishing on a time interval $I = [t_1, t_2]$. During the time interval I, we say that the trajectory is singular, i.e. in closed loop with the singular control D_c to be determined. Firstly, from (12), we get:

$$\begin{aligned} \dot\lambda_1 &= -\frac{\partial(\rho_1(s) - \mu_1(q_1)q_1)}{\partial q_1}\lambda_1 - \frac{\partial \rho_2(s)}{\partial q_1}\lambda_2 - \frac{\partial \mu_1(q_1)}{\partial q_1}x_1\lambda_3, \\ \dot\lambda_2 &= -\frac{\partial \rho_1(s)}{\partial q_2}\lambda_1 - \frac{\partial(\rho_2(s) - \mu_2(q_2)q_2)}{\partial q_2}\lambda_2 - \frac{\partial \mu_2(q_2)}{\partial q_2}x_2\lambda_4, \\ \dot\lambda_3 &= -\frac{\partial \rho_1(s)}{\partial x_1}\lambda_1 - \frac{\partial \rho_2(s)}{\partial x_1}\lambda_2 - \mu_1(q_1)\lambda_3 + \lambda_3 D, \\ \dot\lambda_4 &= -\frac{\partial \rho_1(s)}{\partial x_2}\lambda_1 - \frac{\partial \rho_2(s)}{\partial x_2}\lambda_2 - \mu_2(q_2)\lambda_4 + \lambda_4 D. \end{aligned}$$

Using $s_{in} = s + x_1q_1 + x_2q_2$, and the notations: $\rho_i'(s) = \frac{\partial \rho_i(s)}{\partial s}$, and, $\tilde\mu_i'(q_i) = \frac{\partial \mu_i(q_i)q_i}{\partial q_i}$, (in the case where μ_i given by (4), we get, $\tilde\mu_i'(q_i) = \mu_{i\infty}$), we deduce that:

$$\begin{aligned} \dot\lambda_1 &= \rho_1'(s)\lambda_1 x_1 + \mu_{1\infty}\lambda_1 + \rho_2'(s)\lambda_2 x_1 - \mu_1'(q_1)\lambda_3 x_1, \\ \dot\lambda_2 &= \rho_1'(s)\lambda_1 x_2 + \mu_{2\infty}\lambda_2 + \rho_2'(s)\lambda_2 x_2 - \mu_2'(q_2)\lambda_4 x_2, \\ \dot\lambda_3 &= \rho_1'(s)\lambda_1 q_1 + \rho_2'(s)\lambda_2 q_1 - \mu_1(q_1)\lambda_3 + \lambda_3 D, \\ \dot\lambda_4 &= \rho_1'(s)\lambda_1 q_2 + \rho_2'(s)\lambda_2 q_2 - \mu_2(q_2)\lambda_4 + \lambda_4 D. \end{aligned} \tag{17}$$

Now, for all $t \in I$, belonging to $[0, t_f]$, we consider that: $\Phi(t) = -\lambda_3(t)x_1(t) - \lambda_4(t)x_2(t) = 0$. It follows that $\dot\Phi(t) \equiv 0$, for all $t \in I$, and such that for all $t \geq 0$:

$$\dot\Phi = -\,(q_1x_1 + q_2x_2)\underbrace{(\rho_1'(s)\lambda_1 + \rho_2'(s)\lambda_2)}_{\Psi}.$$

Since the system (1) is positive, we deduce that $q_1x_1 + q_2x_2 > 0$, and consequently $\dot\Phi(t) \equiv 0$, for all $t \in I$, gives:

$$\Psi(t) = \rho_1'(s(t))\lambda_1(t) + \rho_2'(s(t))\lambda_2(t) = 0, \;\; \forall t \in I. \tag{18}$$

Similarly, since $\Psi(t) \equiv 0$ for all $t \in I$, it follows that $\dot\Psi(t) \equiv 0$ on the same time interval. We readily check that:

$$\dot\Psi = (\rho_1''(s)\lambda_1 + \rho_2''(s)\lambda_2)\,\dot s + \underbrace{\rho_1'(s)\dot\lambda_1 + \rho_2'(s)\dot\lambda_2}_{\xi}, \tag{19}$$

for all $t \geq 0$. Using $\dot\lambda_1$ and $\dot\lambda_2$, given in (17), ξ reads:

$$\begin{aligned} \xi =&[\rho_1'(s)]^2\lambda_1 x_1 + \rho_1'(s)\lambda_1\tilde\mu_1'(q_1) \\ &+ \rho_1'(s)\rho_2'(s)\lambda_2 x_1 - \rho_1'(s)\mu_1'(q_1)\lambda_3 x_1 \\ &+ \rho_1'(s)\rho_2'(s)\lambda_1 x_2 + \rho_2'(s)\lambda_2\tilde\mu_2'(q_2) \\ &+ [\rho_2'(s)]^2\lambda_2 x_2 - \rho_2'(s)\mu_2'(q_2)\lambda_4 x_2. \end{aligned} \tag{20}$$

Since, on the singular arc, we have $\lambda_3 x_1 = -\lambda_4 x_2$, and, $\rho_1'(s)\lambda_1 = -\rho_2'(s)\lambda_2$, we end up with:

$$\begin{aligned} \xi =&\rho_1'(s)\left[\tilde\mu_1'(q_1) - \tilde\mu_2'(q_2)\right]\lambda_1 \\ &- x_1\left[\rho_1'(s)\mu_1'(q_1) - \rho_2'(s)\mu_2'(q_2)\right]\lambda_3, \end{aligned} \tag{21}$$

where $\rho_i'(s) = \frac{\rho_{im}K_{si}}{(K_{si}+s)^2}$ and $\rho_i''(s) = -\frac{2\rho_{im}K_{si}}{(K_{si}+s)^3}$.

Now, we are ready to determine the expression of the singular control D_c for all $t \in I$. For that, we use (18), (19), (21), and we extract the expression of the control D_c at any time $t^\dagger \in I$, depending on whether $\xi(t^\dagger)$ and the term multiplying $\dot s$ in (19) are zero or not. In fact, in the general case, these terms are different from zero and the singular control is given by (A.2) (see, case ① in Appendix A). An interesting case holds when $\xi \equiv 0$, since it gives a simpler expression for D_c, given by (A.4) (see case ② in Appendix A). In numerical simulations, we have noticed that ξ is in the general case significantly large. However, this does not prevent the control given in (A.4) (case ②) from being a good approximation of the control

[2] The overscript tr means the transpose of the vector/matrix.

given in (A.2) (case ①). In fact, we claim that the control (A.4) is a sub-optimal control that can be more useful in practical implementation than the optimal control given in (A.2). It is also worth mentioning that the control given in (A.4) is in fact the generalization of the singular control obtained for Monod's model (Bayen & Mairet (2014)). Finally, the case ③ in Appendix A corresponds to the particular case in which $\rho_1''(s)\lambda_1 + \rho_2''(s)\lambda_2 = 0$. We are at least sure that this case holds at the final time t_f, due to the transversality conditions (15), however, since it holds on a singular time-instant, we consider that the control in (A.9) is less significant than the two previous ones.

To summarize, we applied in this section the Pontryagin's principle in order to get some insights on the form of the optimal control in our specific optimization problem, which could combine bang-type controls (0 and/or $D_{\max}$), as well as singular arcs D_c (given by (A.2)). We further know that the target is reached with $\Phi(t_f) = 0$, thanks to the transversality conditions. Now, we are going to determine the structure of the optimal control using a direct method, i.e. by discretizing the optimal control problem and solving a nonlinear programming problem (Betts (2010), Biergler (2010)).

5. A NUMERICAL OPTIMAL SYNTHESIS

In this section, a numerical optimal synthesis is carried out on the Droop's model (1), with the biological parameters and functions given in Table 1. The direct method that we apply is implemented in the `Bocop` software [3] (see, e.g., Bonnans *et al.* (2017)), which solves nonlinear optimization problems using some interior point approaches. More precisely, we use a discontinuous collocation method of Lobatto's type (a sixth order time-discretization Labatto IIIC formula), with a time-discretization of 500 steps. In the settings of the optimization problem, we consider a free final-time t_f and we choose a target $\mathcal{T}$ with a contamination coefficient $\epsilon = 0.3$.

Table 1. Parameters of the numerical example.

i	$k_{qi}(\mu mol^3/L)$	$\mu_{i\infty}(day^{-1})$	$K_{si}\,(\mu mol/L)$
1	0.35	0.9	0.1
2	0.2	0.75	0.7

i	$\rho_{im}(\mu mol/\mu m^3/day)$	$s_{in} = 2\,(\mu mol/L)$
1	0.88	
2	0.95	

At a first glance, the numerical results that we obtain suggest that the optimal strategy aims, in a first step, to drive the system from the initial condition s^0 of the substrate s around the value $s = s_c$ (but not exactly to s_c, as illustrated in the sequel). We can interpret this behavior by saying that the control aims to put the system in an operating mode that ensures an ability to separate the species as quickly as possible, since s_c maximizes the function $\Delta(s) = \mu_1(\delta^{-1}(s)) - \mu_2(\delta^{-1}(s))$. Then, in a second phase, the singular arc – or singular control D_c – steers the states x_i to the target $\mathcal{T}$ in minimal time. It is worth mentioning that this *bang-singular* type control is similar to the one observed in Monod's model (Bayen & Mairet (2014)), with the notable exception that the substrate s is no longer constant along the singular arc in our case. More importantly, the switching instant, that we denote t_s throughout this section, does not correspond to $s(t_s) = s_c$, as it was the case in the simpler Monod's model (Bayen & Mairet (2014)). The characterization of the switching instant t_s proves to be a challenging issue in our optimization problem and it deserves a separated study. However, we highlight in this work the link between the switching instant t_s and the dynamics of the co-state of the substrate s. In fact, we recall that we did not focus in the previous section on the s-dynamics as well as its co-state, thanks to the features of the set $\mathcal{F}$ (Proposition 1). However, we mention here that t_s corresponds to the time at which the co-state of s becomes zero, and it remains zero for all $t \in [t_s, t_f]$. Admittedly, it is not always possible to interpret the dynamics of the co-states; however, in this case, the co-state of s is zero on $[t_s, t_f]$, meaning that $s(t) \equiv s^\star(t)$, for all $t \in [t_s, t_f]$, where there is no gain in changing the dynamics $s \equiv s^\star$ on that interval. Furthermore, in the simple case of Monod's model, it appears that the optimal trajectory $s^\star(t)$ for $t \in [t_s, t_f]$ coincides with the constant that is equivalent to s_c in Droop's model. The previous observation (from Bayen & Mairet (2014)) seems quite natural in Monod's model. However, Droop's model is less trivial to interpret since the variables q_i introduce a latency (i.e. they act as time-delays) between the absorption of s and the growth of the species x_i, in a nontrivial way. Thus, the model achieves better performance through $s^\star$ (that we characterize via the co-state of s), than s_c. This being so, we focus in the sequel on the following two cases that summarize the numerical optimal synthesis:

❶ If $s^0 > s_c$, the control steers s to the vicinity of s_c and it is initially set to its minimal value, i.e. $D = 0$, during this first phase. When $D = 0$, we get from the model equations: $\dot{s} < 0$ and the s variable decreases. It is possible that the trajectories reach the target $\mathcal{T}$ (this depends for instance on x_i^0); however, in the general case, we observe that the phase *bang(0)* is followed by a singular phase, where the control $D = 0$ switches to the singular control D_c in (A.2), which steers the trajectories to the target $\mathcal{T}$ later on.

❷ If $s^0 < s_c$, the control steers s to the vicinity of s_c and it is maximum, i.e. $D = D_{\max}$, during the first phase. Similarly to the previous case, it is possible that the system reaches the target after some time. However, in the general case, we notice that there exists a switching instant t_s at which the control becomes singular. This singular arc steers the trajectories to the target $\mathcal{T}$ in minimal time. Let us observe that the dynamics of x_i in closed loop with $D = D_{\max}$ are governed by: $\dot{x}_i = [\mu_i(q_i) - D_{\max}]\, x_i$. We deduce that the biomass species concentrations x_i converge exponentially to zero when $D_{\max}$ is sufficiently large (e.g. $D_{\max} = 1 > \mu_{mi}$ in the numerical example). It follows that s converges to s_{in} when $t \to \infty$. Thus, s increases and approaches $s_c \in [0, s_{in}]$ in finite time.

The behaviors outlined in ❶ and ❷ are highlighted in the rest, starting from numerical simulations performed when the initial conditions are given by: $s^0 = 1$, $x_1^0 = x_2^0 = 0.5$, $q_1^0 = q_2^0 = 1$, within the invariant set $\mathcal{F}$.

The optimal control provided by Bocop in this case is given in Figure 3. The structure *bang(0)-singular* of the

[3] `Bocop` is an optimal control solver, `https://www.bocop.org/`

control is validated by checking that the functions Φ and $\dot{\Phi}$ are zero in this case. In addition, we check that the control on the singular arc shown in Figure 3 corresponds to the control determined in (A.2) (see the figure given in Appendix A). Next, the corresponding model trajectories are given in Figure 4. The switching time instant t_s is characterized by the co-state of the s variable, as illustrated in Figure 5. Finally, the function $\Delta(s(t))$, $\forall t \in [0, t_f]$, is shown in Figure 6.

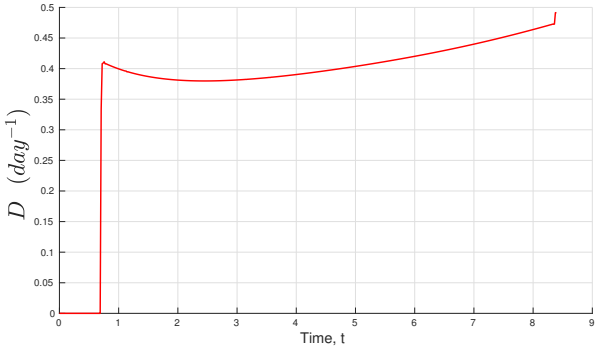

Fig. 3. The optimal control provided by Bocop when $s^0 = 1 > s_c$ is a *bang(0)-singular* control law.

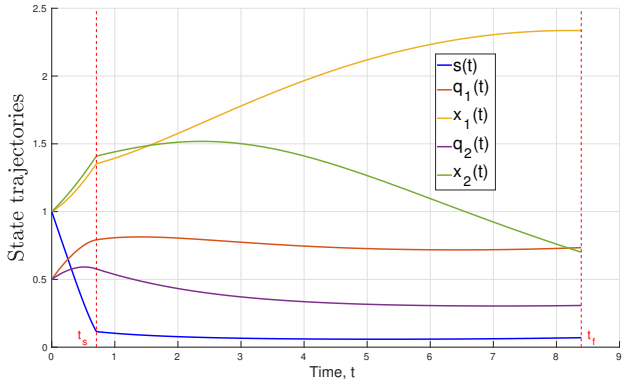

Fig. 4. Trajectories associated to the initial conditions $s^0 = 1$, $x_1^0 = x_2^0 = 0.5$, $q_1^0 = q_2^0 = 1$, in closed loop with the *bang(0)-singular* control law in Figure 3.

In Figure 4, we notice that the substrate s is not constant on the singular arc, but it remains in the vicinity of s_c (see also Figure 6, where we observe that $\Delta(s)$ evolves suboptimally on the singular arc).
In a similar way, we can check that if $s^0 < s_c$ (i.e. as in situation ❷), then the optimal control is *bang-singular*, where this time the bang corresponds to $D = D_{\max}$.

Now, we consider the initial conditions: $s^0 = 0.02$, $x_1^0 = x_2^0 = 1.2375$, $q_1^0 = q_2^0 = 0.8$, within the invariant set $\mathcal{F}$. We also set the upper bound on the control at $D_{\max} = 1$. The optimal control in this case is given in Figure 7. The dynamics of the substrate s, in closed loop with that control, is shown in Figure 8. The trajectories of the whole state vector are illustrated in Figure 9. As previously mentioned, the switching instant t_s is identified from the co-state of the substrate s, as indicated in Figure 10.

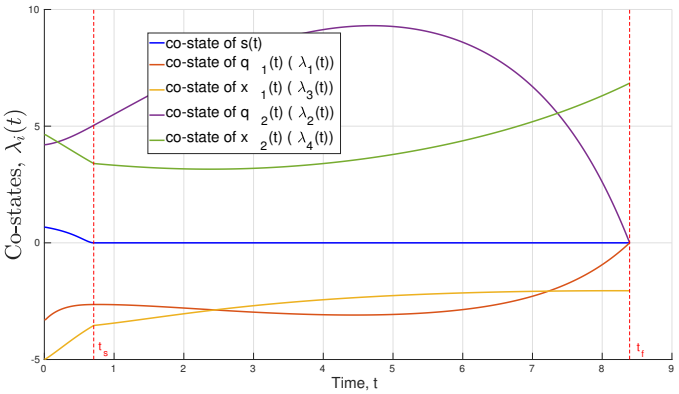

Fig. 5. Co-states trajectories for all $t \in [0, t_f]$. We notice that the switching time corresponds to the instant at which the co-state of s becomes zero. The co-state of the s-dynamics remains zero until reaching t_f, i.e. until the trajectories reach the target $\mathcal{T}$.

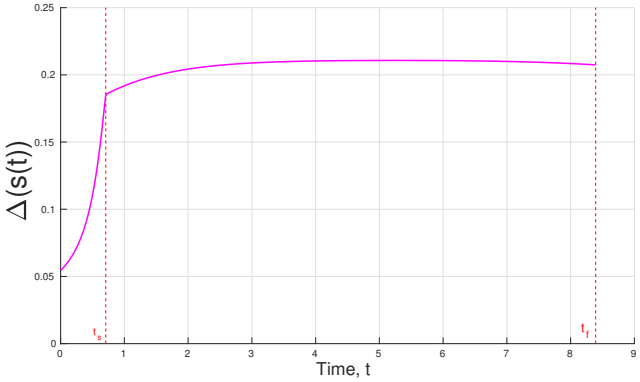

Fig. 6. Evolution of the function $\Delta(s(t))$, evaluated along the optimal trajectory $s(t)$, for all $t \in [0, t_f]$.

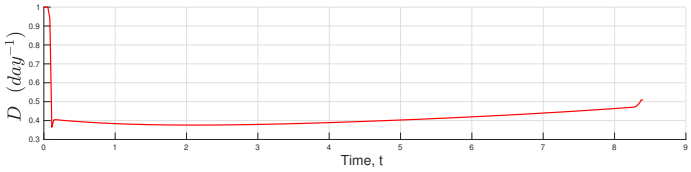

Fig. 7. The optimal control in the case where $s^0 < s_c$ is of type *bang(1)-singular*.

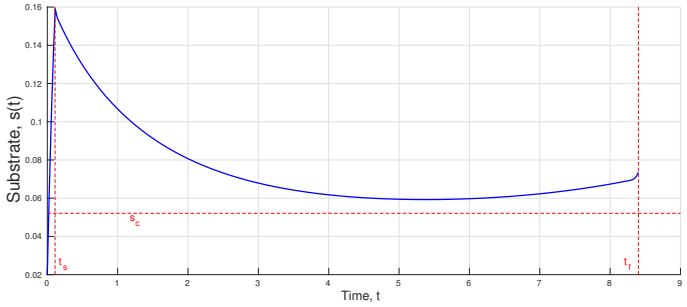

Fig. 8. The optimal substrate trajectory for all $t \in [0, t_f]$, starting from the initial condition $s^0 = 0.02$.

6. CONCLUSION

In this work, we have investigated the issue of minimal-time selection of microalgae species. From the insights

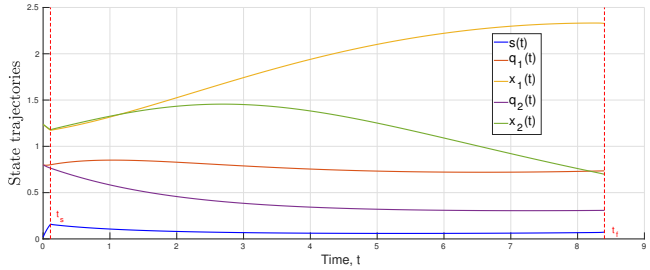

Fig. 9. Trajectories associated to: $s^0 = 0.02$, $x_1^0 = x_2^0 = 1.2375$, $q_1^0 = q_2^0 = 0.8$, in closed loop with the *bang(1)-singular* control law in Figure 7.

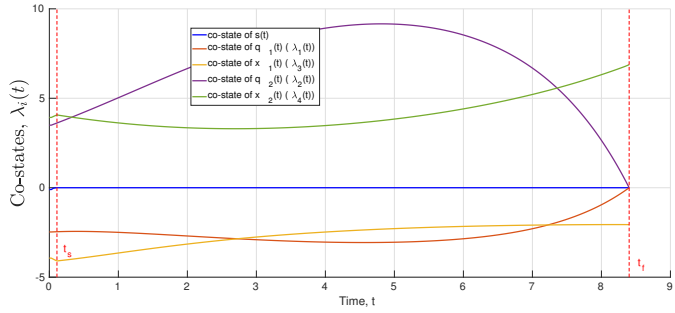

Fig. 10. Trajectories of the co-states for all $t \in [0, t_f]$.

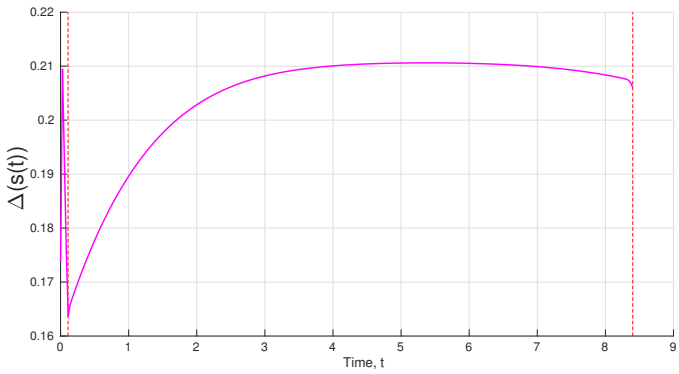

Fig. 11. Evolution of the function $\Delta(s(t))$, evaluated along the optimal trajectory $s(t)$, for all $t \in [0, t_f]$.

given by Pontryagin's principle, and using a direct method for the optimization problem, we highlighted in this paper the fact that the optimal feedback law is of type *bang-singular*, where the switching time is related to the dynamics of the co-state of the substrate, and the bangs are of two types (0 and $D_{\max}$) depending on the substrate initial state. In future work, we will focus on the deepening of the optimal synthesis, which is proving hardly tractable for a chemostat system involving five states. In particular, we want to investigate the co-states dynamics in order to fully characterize the switching instant and the transitions in the control.

ACKNOWLEDGEMENTS

We would like to thank Pierre Martinon and Jean-Baptiste Pomet for the stimulating discussions we had on the topic.
This work was supported by the *IPL Algae in silico*, Inria Project Lab, France.

REFERENCES

T. Bayen, & F. Mairet, *Optimization of the separation of two species in a chemostat.* Automatica, 50(4), pp. 1243-1248, (2014).

T. Bayen, & F. Mairet, *Optimization of strain selection in evolutionary continuous culture.* International Journal of Control, 90(12), pp. 2748-2759, (2017).

O. Bernard, F. Mairet, B. Chachuat, *Modelling of microalgae culture systems with applications to control and optimization.* Microalgae Biotechnology. Springer, Cham, pp. 59-87, (2015).

O. Bernard, *Hurdles and challenges for modelling and control of microalgae for CO2 mitigation and biofuel production.* Journal of Process Control 21, no. 10, pp. 1378-1389, (2011).

J. T. Betts, *Practical methods for optimal control and estimation using nonlinear programming.* Siam, Advances in Design & Control, 2nd Edition, Vol. 19, p. 427, (2010).

L. T. Biergler, *Nonlinear Programming: Concepts, Algorithms, and Applications to Chemical Processes.* MPS-SIAM Series on Optimization (Book 10), SIAM-Society for Industrial and Applied Mathematics, p. 415, (2010).

F. J. Bonnans, D. Giorgi, V. Grelard, B. Heymann, S. Maindrault, P. Martinon, O. Tissot, J. Liu, *BOCOP: an open source toolbox for optimal control - A collection of examples.* Team Commands, Inria Saclay, Technical Reports, `http://bocop.org`, (2017).

J. Caperon, & J. Meyer, *Nitrogen-limited growth of marine phytoplanktonII. Uptake kinetics and their role in nutrient limited growth of phytoplankton.* In Deep Sea Research and Oceanographic Abstracts, Vol. 19, No. 9, pp. 619-632, (1972).

M. R. Droop, *Vitamin B_{12} and marine ecology. IV. The kinetics of uptake growth and inhibition in Monochrysis lutheri.* J. Mar. Biol. Assoc. 48 (3), pp. 689-733, (1968).

M. R. Droop, *Some thoughts on nutrient limitation in algae.* Journal of Phycology, 9(3), pp.264-272, (1973).

M. R. Droop, *25 years of algal growth kinetics, a personal view.* Bot. Mar. 16, pp. 99-112, (1983).

F. Grognard, P. Masci, E. Benoît, O. Bernard, *Competition between phytoplankton and bacteria: exclusion and coexistence.* J. of Math. Bio., 70(5), pp. 959-1006, (2015).

L. M. Hocking, *Optimal control: an introduction to the theory with applications.* Oxford University Press, (1991).

S. B. Hsu, & T. H. Hsu, *Competitive exclusion of microbial species for a single nutrient with internal storage.* SIAM J. on Applied Math., 68(6), pp.1600-1617, (2008).

S. B. Hsu, S. Hubbell, P. Waltman, *A mathematical theory for single-nutrient competition in continuous cultures of microorganisms.* SIAM Journal on Applied Mathematics, Vol. 32, No. 2, pp. 366-383, (1977).

S. Liu, *Bioprocess Engineering: Kinetics, Sustainability, and Reactor Design.* 2nd Ed., Elsevier, p. 1172, (2016).

P. Masci, O. Bernard, F. Grognard, *Continuous selection of the fastest growing species in the chemostat.* IFAC World Congress, IFAC Proceedings, 41(2), pp.9707-9712, (2008).

F. Mazenc & M. Malisoff, *Stabilization of a chemostat model with Haldane growth functions and a delay in the measurements.* Automatica, 46(9), pp.1428-1436, (2010).

J. Monod, *Recherches sur la croissance des cultures bactériennes.* Paris: Herman., (1942).

J. Monod, *La technique de culture continue; théorie et applications.* Annales de l'Institute Pasteur 79: pp. 390-401, (1950).

L. S. Pontryagin, V. G. Boltyanskiy, R. V. Gamkrelidze, E. F. Mishchenko, *Mathematical theory of optimal processes.* New York, NY Springer, (1964).

H. L. Smith, & P. Waltman, *The theory of the chemostat: dynamics of microbial competition.* Cambridge Studies in Mathematical Biology, Cambridge Univ. Press, (1995).

Appendix A. DETERMINATION OF THE SINGULAR CONTROL FEEDBACK, ON SINGULAR ARCS

We use the equation (19) and the fact that $\dot{\Psi}(t) \equiv 0$ for all $t \in I = [t_1, t_2]$. From the dynamics of the substrate s, given in the system (1), we conclude that:

① If

$$\rho_1''(s(t^\dagger))\lambda_1(t^\dagger) + \rho_2''(s(t^\dagger))\lambda_2(t^\dagger) \neq 0, \quad \text{and,} \quad \xi(t^\dagger) \neq 0, \tag{A.1}$$

then, we deduce that:

$$D_c(t^\dagger) = \frac{\left(\rho_1(s(t^\dagger))x_1(t^\dagger) + \rho_2(s(t^\dagger))x_2(t^\dagger)\right)\left(\rho_1''(s(t^\dagger))\lambda_1(t^\dagger) + \rho_2''(s(t^\dagger))\lambda_2(t^\dagger)\right) - \xi(t^\dagger)}{(s_{in} - s(t^\dagger))\left(\rho_1''(s(t^\dagger))\lambda_1(t^\dagger) + \rho_2''(s(t^\dagger))\lambda_2(t^\dagger)\right)}. \tag{A.2}$$

② If

$$\rho_1''(s(t^\dagger))\lambda_1(t^\dagger) + \rho_2''(s(t^\dagger))\lambda_2(t^\dagger) \neq 0, \quad \text{and,} \quad \xi(t^\dagger) = 0, \tag{A.3}$$

then, we deduce that $\dot{s}(t^\dagger) = 0$ and

$$D_c(t^\dagger) = \frac{\rho_1(s(t^\dagger))x_1(t^\dagger) + \rho_2(s(t^\dagger))x_2(t^\dagger)}{s_{in} - s(t^\dagger)}. \tag{A.4}$$

③ If

$$\rho_1''(s(t^\dagger))\lambda_1(t^\dagger) + \rho_2''(s(t^\dagger))\lambda_2(t^\dagger) = 0, \tag{A.5}$$

then, we deduce that $\dot{\Psi}(t^\dagger) = 0$ implies that $\xi(t^\dagger) = 0$. In this case, we need to compute $\dot{\xi}$ in order to determine the control D_c. It is however worth mentioning that in this case, the following holds at $t = t^\dagger$:

$$\begin{pmatrix} \rho_1'(s) & \rho_2'(s) \\ \rho_1''(s) & \rho_2''(s) \end{pmatrix} \begin{pmatrix} \lambda_1 \\ \lambda_2 \end{pmatrix} = \begin{pmatrix} 0 \\ 0 \end{pmatrix} \tag{A.6}$$

Using the expression of ρ_i, we can check that:

$$\begin{vmatrix} \rho_1'(s) & \rho_2'(s) \\ \rho_1''(s) & \rho_2''(s) \end{vmatrix} \neq 0, \quad \text{for all} \quad K_{s1} \neq K_{s2}. \tag{A.7}$$

If follows that (A.6) is satisfied when $\lambda_1(t^\dagger) = \lambda_2(t^\dagger) = 0$. We will see later that in fact this situation holds for $t^\dagger = t_f$. Thus, in order to determine the singular control in case ③, we proceed as follows. Using $\rho_1''(s)\lambda_1 = -\rho_2''(s)\lambda_2$ and $x_1\lambda_3 = -x_2\lambda_4$, and noticing that on the singular arc we get necessarily: $\dot{\overbrace{\lambda_3 x_1}} = 0$, we conclude that in this case:

$$\dot{\xi} = \Omega(s, q_i, x_i, \lambda_i)\dot{s} + \tilde{\Omega}(s, q_i, x_i, \lambda_i), \tag{A.8}$$

where,

$$\begin{aligned} \Omega(s, q_i, x_i, \lambda_i) &= (\mu_{1\infty} - \mu_{2\infty})\,\rho_1''(s)\lambda_1 - (\rho_1''(s)\mu_1'(q_1) - \rho_2''(s)\mu_2'(q_2))\,\lambda_3 x_1, \\ \tilde{\Omega}(s, q_i, x_i, \lambda_i) &= [\mu_{1\infty}\lambda_1 - \mu_1'(q_1)\lambda_3 x_1]\,\mu_{1\infty}\rho_1'(s) + [\mu_{2\infty}\lambda_2 - \mu_2'(q_2)\lambda_4 x_2]\,\mu_{2\infty}\rho_2'(s) \\ &\quad - \rho_1'(s)\mu_1''(q_1)\lambda_3 x_1\,(\rho_1(s) - \mu_1(q_1)q_1) - \rho_2'(s)\mu_2''(q_2)\lambda_4 x_2\,(\rho_2(s) - \mu_2(q_2)q_2)\,. \end{aligned}$$

Observe that $\dot{\xi} = 0$ gives:

$$D_c = \frac{(\rho_1(s)x_1 + \rho_2(s)x_2)\,\Omega(s, q_i, x_i, \lambda_i) - \tilde{\Omega}(s, q_i, x_i, \lambda_i)}{(s_{in} - s)\Omega(s, q_i, x_i, \lambda_i)}. \tag{A.9}$$

We notice that $\Omega(t_f) \neq 0$ almost everywhere. However, if it happens that $\Omega(t_f) = 0$, we need to derive one more time in order to determine the singular control.

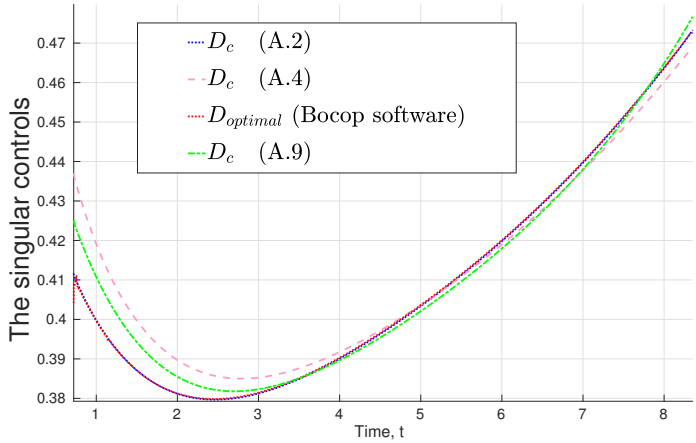

The figure above gives a comparison between the optimal control – in red, from Bocop – on the singular arc, which corresponds to the one in Figure 3, and the theoretical expressions of D_c given in Appendix A. We notice that D_c in (A.2) fits well the optimal control given by Bocop. We have noticed in simulations that the controls given by (A.9) – which corresponds to the singular control at $t = t_f$ since $\lambda_3(t_f) = \lambda_4(t_f) = 0$ – and (A.4) are good approximations of the singular control in (A.2).